Deeply Virtual Compton Scattering with CLAS12 at Jefferson Laboratory

Adam HOBART on behalf of CLAS Collaboration

3D Structure of the Nucleon via Generalized Parton Distributions, Incheon, Korea

Belitsky, Radyushkin, Physics Reports, 2005

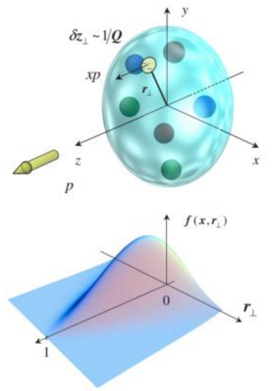

- QCD at low energies: non perturbative regime
  - Need structure functions to describe nucleon structure

GPDs

Correlation of transverse position and longitudinal momentum of partons in the nucleon & the spin structure - through Ji's sum rule X. Ji, Phy.Rev.Lett.78,610(1997)

- GPDs can be accessed through exclusive leptoproduction reactions
- At leading order QCD, chiral-even (quark helicity is conserved), quark sector: 4 GPDs for each quark flavor $H, \widetilde{H}, E$ and $\widetilde{E}$
- GPDs depend on x, ξ and t = (p' − p) 2

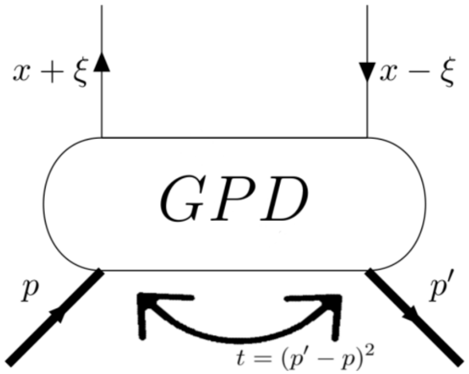

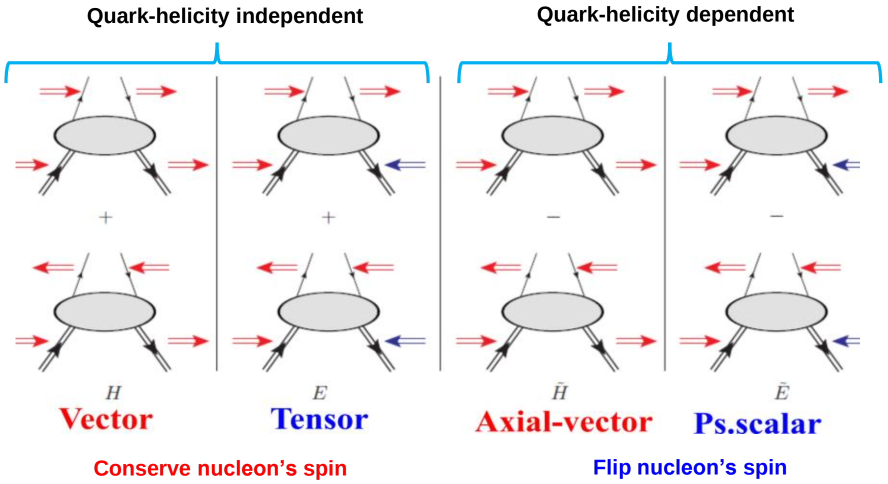

Why are GPDs important?

- GPDs: Fourier transforms of non-local, non-diagonal QCD operators

Nucleon tomography

M. Burkardt, PRD 62, 71503 (2000)

$$q(x,b_\perp) = \int_0^\infty \frac{d^2\Delta_\perp}{(2\pi)^2} e^{i\Delta_\perp b_\perp} H(x,0,-\Delta_\perp^2)$$

$$\Delta q(x,b_\perp) = \int_0^\infty \frac{d^2\Delta_\perp}{(2\pi)^2} e^{i\Delta_\perp b_\perp} \tilde{H}(x,0,-\Delta_\perp^2)$$

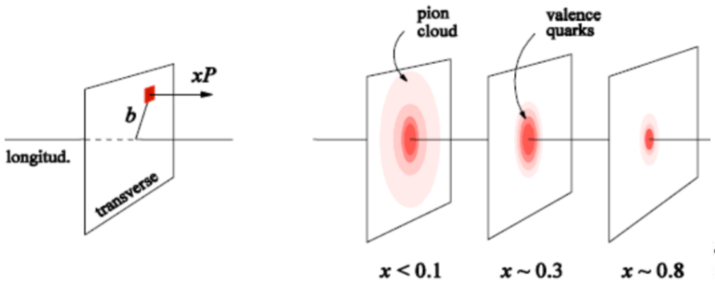

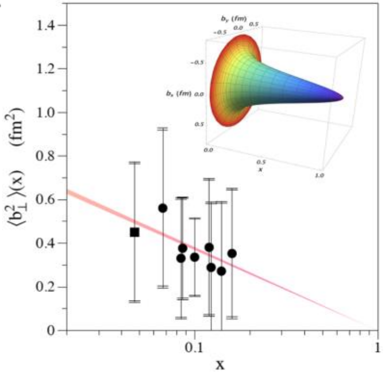

R. Dupré, M. Guidal, M.Vanderhaeghen, PRD95, 011501 (2017)

Quark angular momentum

X. Ji, Phy.Rev.Lett.78,610(1997)

$$\frac{1}{2}\int_{-1}^{1} x dx (H(x,\xi,t=0) + E(x,\xi,t=0)) = J = \frac{1}{2}\Delta\Sigma + \Delta L$$

Nucleon spin: $\frac{1}{2} = \frac{1}{2}\Delta\Sigma + \Delta L + \Delta G$

- The intrinsic spin of the quarks can not explain the origin of the spin of the nucleon **(nucleon Spin Crisis)**
- **Intrinsic spin of the gluons**
- GPDs: quantify the contribution of orbital angular momentum of quarks to the nucleon spin

Deeply Virtual Compton Scattering of leptons off nucleons

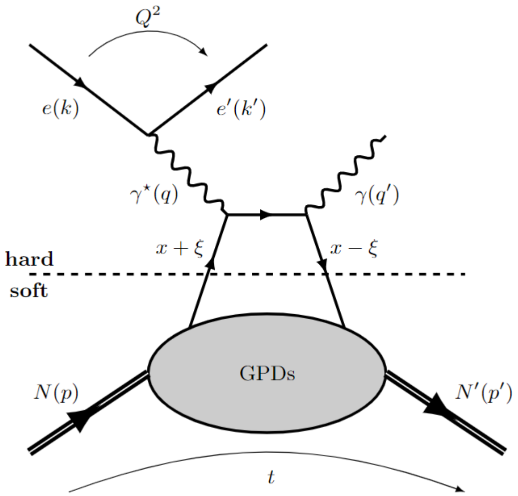

- DVCS allows access to 4 complex GPDs-related quantities:
    - Compton Form Factors (x, ξ,t) (CFFs)

$$\mathcal{H} = \sum_q e_q^2 \left\{ i\,\pi \left[H^q(\xi,\xi,t) - H^q(-\xi,\xi,t) \right] + \mathcal{P}\int_{-1}^{1} dx H^q(x,\xi,t) \left[\frac{1}{\xi - x} - \frac{1}{\xi + x} \right] \right\}$$

- x can not be accessed experimentally by DVCS: Models needed to map the x dependence

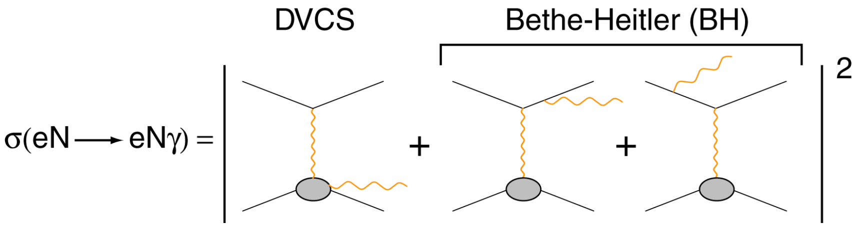

BH is purely electromagnetic and parametrised by FFs

- Experimentally measured observables:
    - Sensitive to the DVCS-BH interference part (linear in CFFs)
        - Should have: Beam polarized and/or target polarized
    - Access to a combinations of CFFs
        - The separation of CFFs requires the measurement of several observables
    - Depending on the target (proton or neutron): different sensitivity to the CFFs (GPDs)
        - The flavor separation of GPDs requires measurements on both nucleons

$$(H,E)_u(\xi,\xi,t) = \tfrac{9}{15}\left[4(H,E)_p(\xi,\xi,t) - (H,E)_n(\xi,\xi,t)\right]$$

$$(H,E)_d(\xi,\xi,t) = \tfrac{9}{15}\left[4(H,E)_n(\xi,\xi,t) - (H,E)_p(\xi,\xi,t)\right]$$

Polarized beam, unpolarized taget

$\Delta\sigma_{LU} \sim \sin(\phi)\, \Im\{F_1 \boldsymbol{H} + \xi(F_1 + F_2)\boldsymbol{\widetilde{H}} - k\, F_2 \boldsymbol{E} + \ \ldots\}$

Unpolarized beam, polarized target

$\Delta\sigma_{UL} \sim \sin(\phi)\, \Im\left\{F_1\, \boldsymbol{\widetilde{H}} + \xi(F_1 + F_2)\left(\boldsymbol{H} + \frac{x_b}{2}\boldsymbol{E}\right) - \xi k\, F_2 \boldsymbol{\widetilde{E}}\right\}$

polarized beam, longitudinal polarized target

$\Delta\sigma_{LL} \sim (A + B\cos(\phi))\, \Re\{F_1\, \boldsymbol{\widetilde{H}} + \xi(F_1 + F_2)\left(\boldsymbol{H} + \frac{x_b}{2}\boldsymbol{E}\right) + \ \ldots\}$

unpolarized beam, transverse polarized target

$\Delta\sigma_{UT} \sim \cos(\phi)\, \sin(\phi_s - \phi)\, \Im\{k(F_2\, \boldsymbol{H} - F_1 \boldsymbol{E}) + \ \ldots\}$

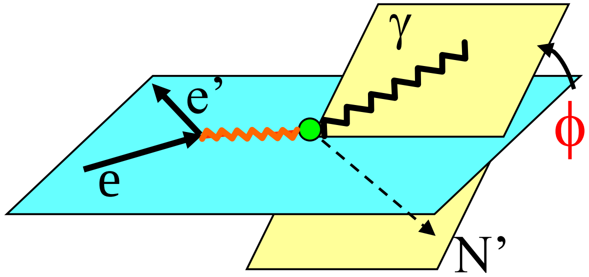

Different contributions from F_1 and F_2 for the different nucleons

Observable	Proton	Neutron
$\Delta\sigma_{LU}$	$\Im\{\boldsymbol{H_p}, \widetilde{H}_p, E_p\}$	$\Im\{H_n, \widetilde{H}_n, \boldsymbol{E_n}\}$
$\Delta\sigma_{UL}$	$\Im\{\boldsymbol{H_p}, \boldsymbol{\widetilde{H}_p}\}$	$\Im\{\boldsymbol{H_n}, E_n\}$
$\Delta\sigma_{LL}$	$\Re\{\boldsymbol{H_p}, \boldsymbol{\widetilde{H}_p}\}$	$\Re\{\boldsymbol{H_n}, E_n\}$
$\Delta\sigma_{UT}$	$\Im\{\boldsymbol{H_p}, \boldsymbol{E_p}\}$	$\Im\{\boldsymbol{H_n}\}$

e.g. (in experiment) $\Delta\sigma_{LU} = \frac{1}{Pol.} \times \frac{N^+ - N^-}{N^+ + N^-}$

- **DVCS with an unpolarized deuterium target :**
- Scattering off neutron (nDVCS): GPD **E**
  - Determination of Ji sum rule
    - Contribution of orbital angular momentum of quarks to the nucleon spin

$$\frac{1}{2}\int_{-1}^{1} xdx(H(x,\xi,t=0)+E(x,\xi,t=0)) = J = \frac{1}{2}\Delta\Sigma + \Delta L$$

- Scattering off proton (pDVCS): GPD **H**
  - Quantify medium effects
    - Essential for the extraction of BSA of a "free" neutron (de-convoluting medium effect via comparison with DVCS on hydrogen target)
- The BSA for nDVCS:
  - is complementary to the TSA for pDVCS on transverse target, aiming at *E*
  - depends strongly on the kinematics → wide coverage needed
  - is smaller than for pDVCS → more beam time needed to achieve reasonable statistics

Different contributions from F_1 and F_2 for the different nucleons

Observable	Proton	Neutron
$\Delta\sigma_{LU}$	$\Im\{\boldsymbol{H_p}, \widetilde{H}_p, E_p\}$	$\Im\{H_n, \widetilde{H}_n, \boldsymbol{E_n}\}$
$\Delta\sigma_{UL}$	$\Im\{\boldsymbol{H_p}, \boldsymbol{\widetilde{H}_p}\}$	$\Im\{\boldsymbol{H_n}, E_n\}$
$\Delta\sigma_{LL}$	$\Re\{\boldsymbol{H_p}, \boldsymbol{\widetilde{H}_p}\}$	$\Re\{\boldsymbol{H_n}, E_n\}$
$\Delta\sigma_{UT}$	$\Im\{\boldsymbol{H_p}, \boldsymbol{E_p}\}$	$\Im\{\boldsymbol{H_n}\}$

Model predictions (VGG) for different values of quarks' angular momentum

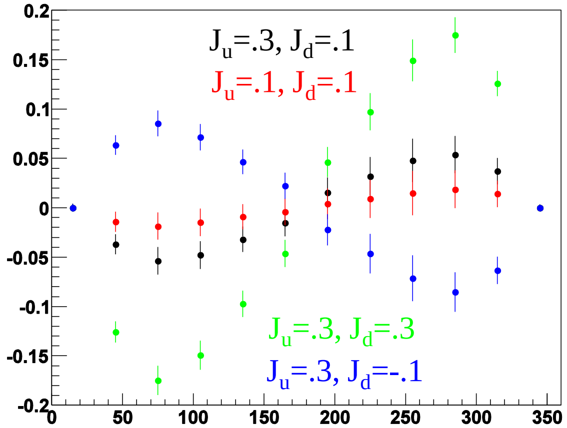

The CEBAF and CLAS at Jefferson Laboratory

Continuos Electron Beam Accelerator Facility

- Up to 12 GeV electrons
- Two anti-parallel linacs, with recirculating arcs on both ends
- 4 experimental halls

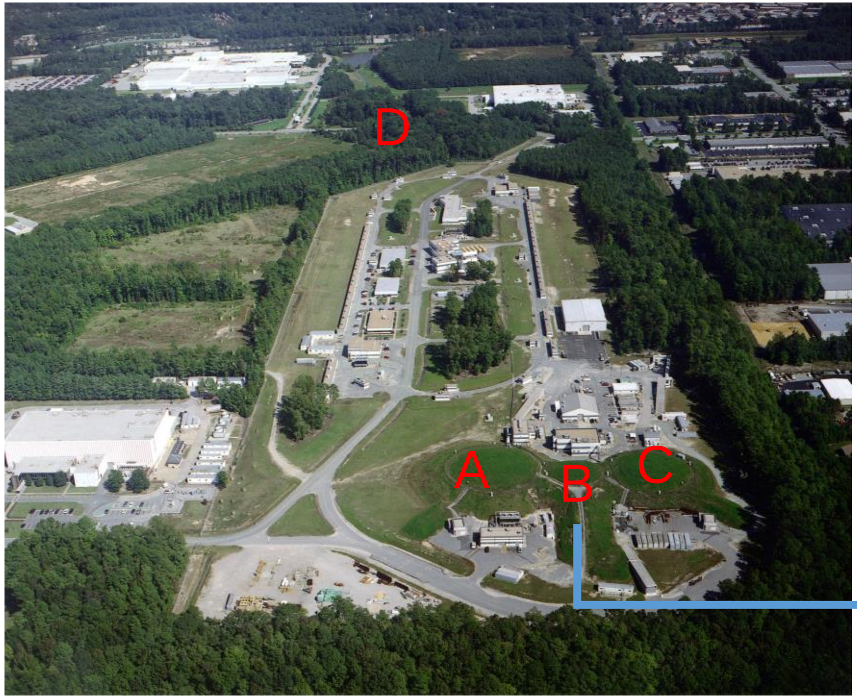

CLAS12

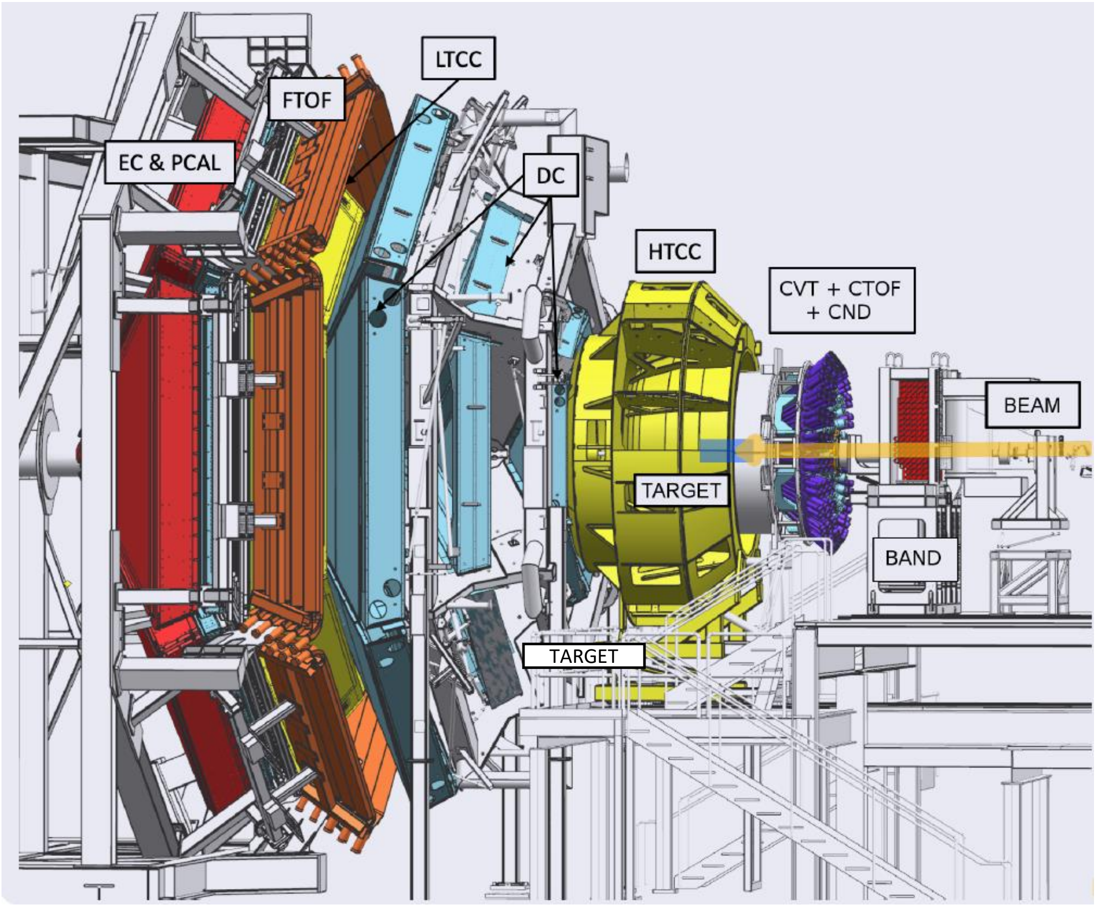

CLAS12: DVCS off proton G. Christiaens, M. Defurne, D. Sokhan Phys. Rev. Lett. 130 (21) 211902 (2023)

- A 10.6 GeV electron beam
  - With an average polarization of 86%
  - Scattering off an unpolarized LH2 target of 5 cm length

The exclusivity of the event is insured by:

Electron detection: Cerenkov detector, drift chambers and electromagnetic calorimeter

Photon detection: sampling calorimeter or a small PbWO4-calorimeter close to the beamline

Proton detection: Silicon and Micromegas detector

- Exclusivity is enforced by cutting on 5 variables:
  - The missing mass ep→eγpX
  - The missing mass ep→eγX
  - The missing energy
  - The missing transverse momentum
  - The cone angle (angle between detected photon and expected photon assuming exclusivity)

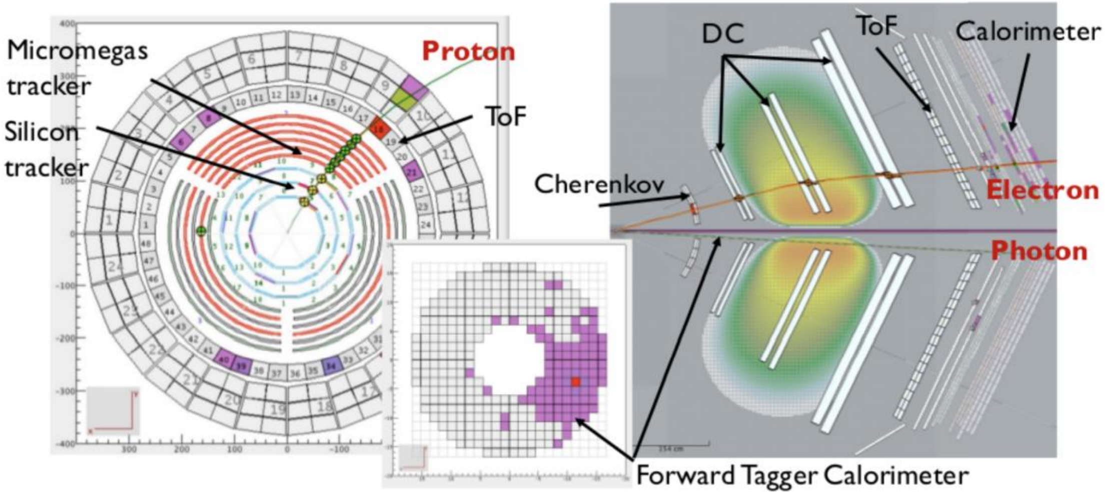

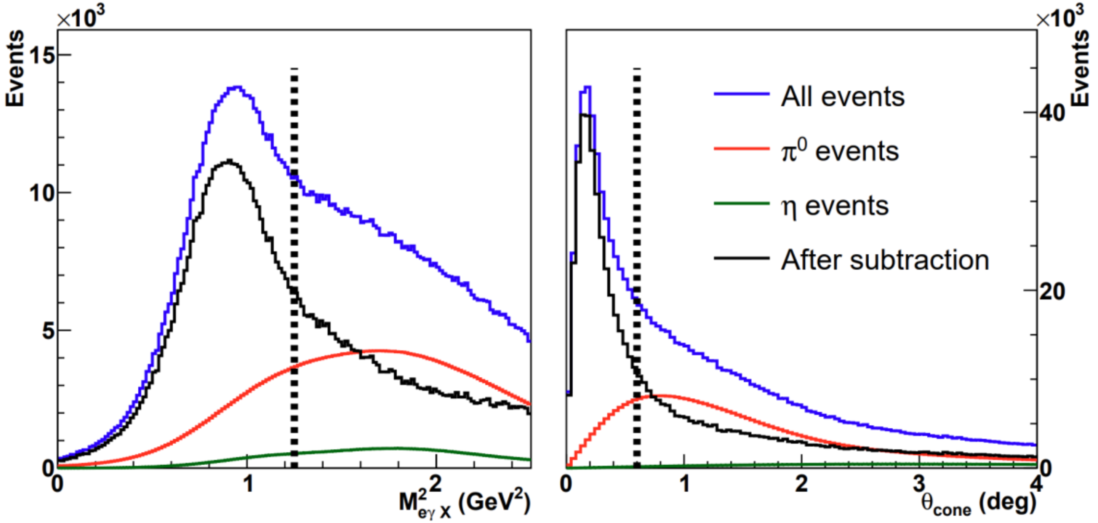

- For each Q^2/x_b, 4 bins in t are defined
  - 64 (Q^2, x_b, t) kinematical bins
- Φ: adaptative binning to accommodate for the steep dependence of the cross section.

(Q^2, x_b, t) kinematics are Φ dependent

- Binning chosen to accommodate for this variation

Wide kinematical coverage

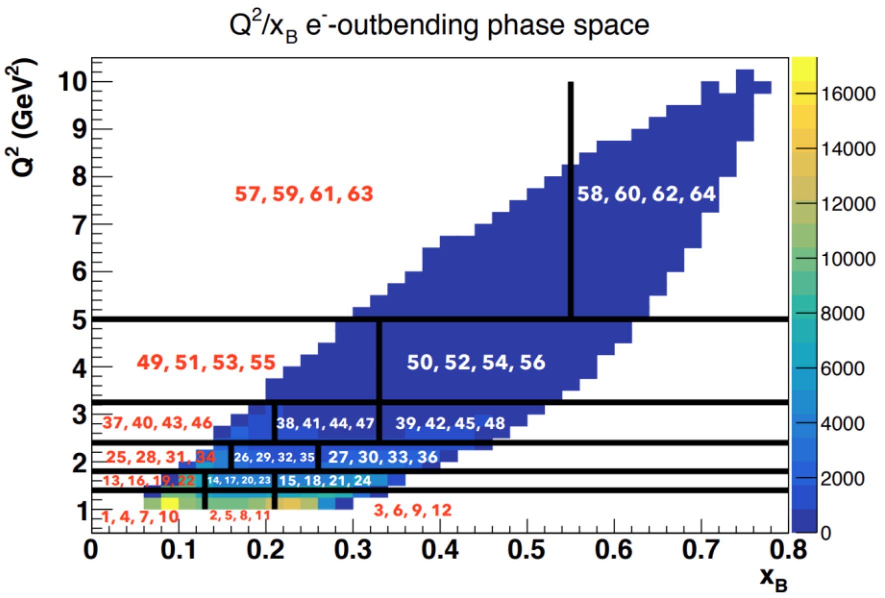

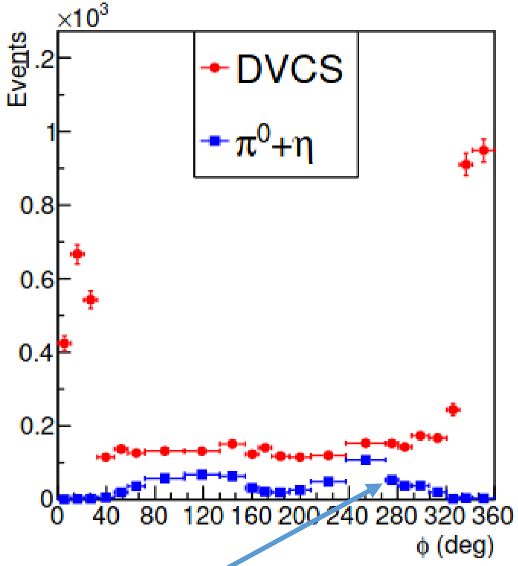

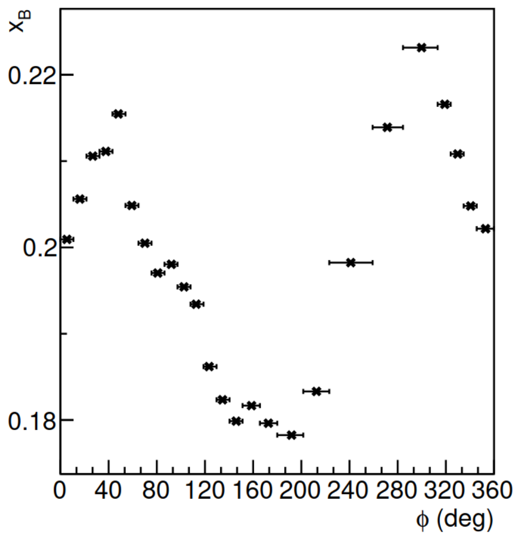

π^0/η background subtraction is insured using toy MC

CLAS12: DVCS off proton G. Christiaens, M. Defurne, D. Sokhan Phys. Rev. Lett. 130 (21) 211902 (2023)

- Deriving the mean and standard deviation of a 100 ANN-predictions produced by a global fit (PARTONS)
  - The new data are shown to be in good agreement
- Comparisons with KM15 and VGG/GK models
  - Data favors the KM15 model for most of the bins
  - At large x_b data favors the VGG/GK models

H. Moutarde, P. Sznajder, and J. Wagner, EPJC 79, 614 (2019)

Kumericki, Kresimir and M uller, Dieter, EPJ Web of Conferences 112, 01012 (2016).
S. V. Goloskokov and P. Kroll, EPJC 65, 10.1140 (2009)
M. Vanderhaeghen, P. A. Guichon, and M. Guidal, Phys.Rev. D60, 094017 (1999)

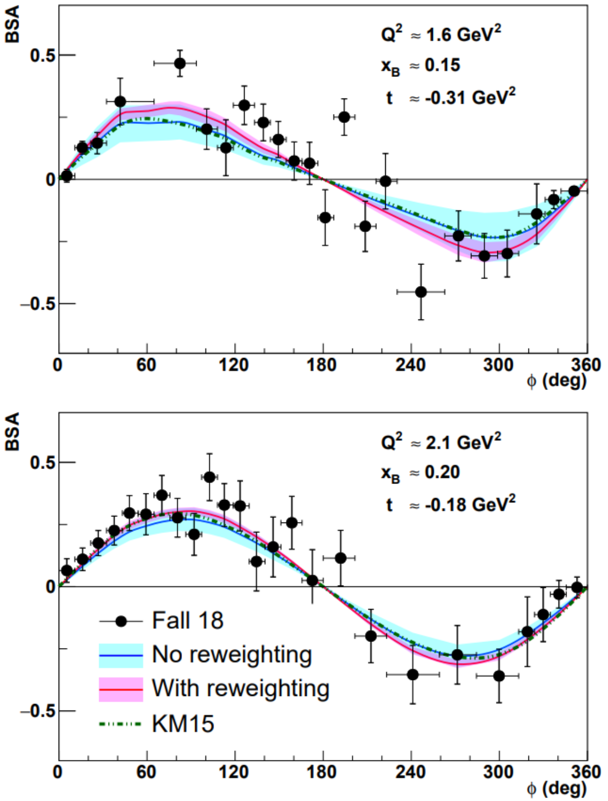

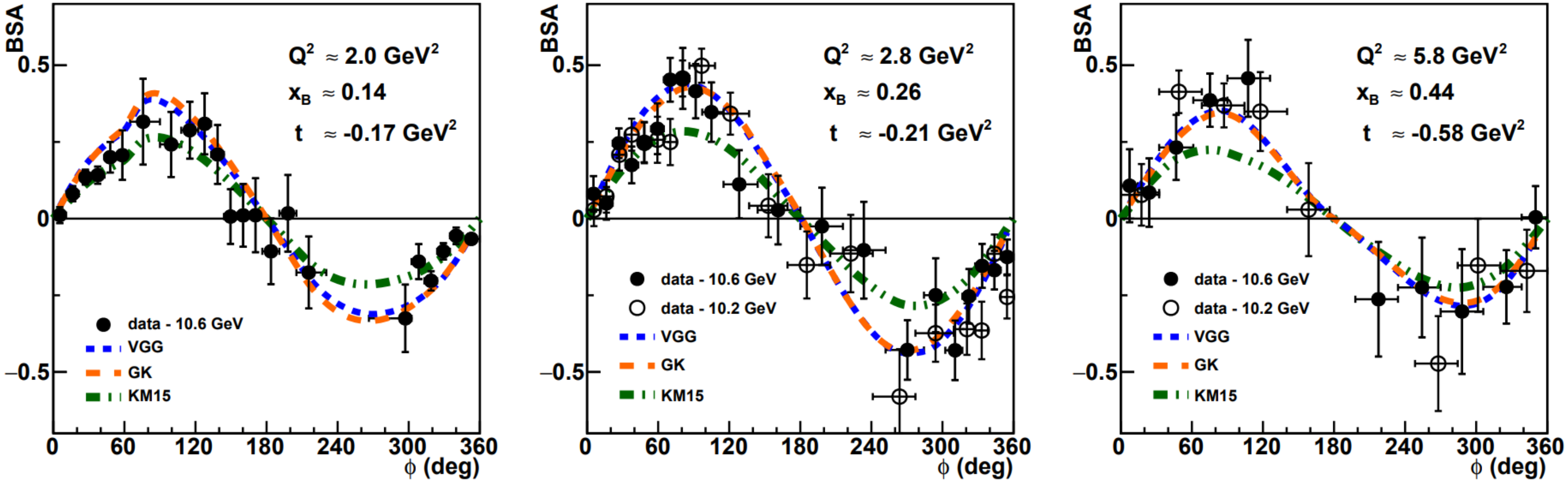

CLAS12: DVCS with an unpolarized deuterium target

- A 10.6/10.4/10.2 GeV electron beam
  - With an average polarization of 86%
  - Scattering off an unpolarized Liquid Deuterium target of 5 cm length
- The exclusivity of the event is insured by:
  - Electron detection: Cerenkov detector, drift chambers and electromagnetic calorimeter
  - Photon detection: sampling calorimeter or a small PbWO4-calorimeter close to the beamline
  - Proton detection: Silicon and Micromegas detector OR Neutron detection: Central Neutron Detector
- For Neutron Detection:
  - Machine Learning techniques are applied to improve the Identification and reduce charged particle contamination

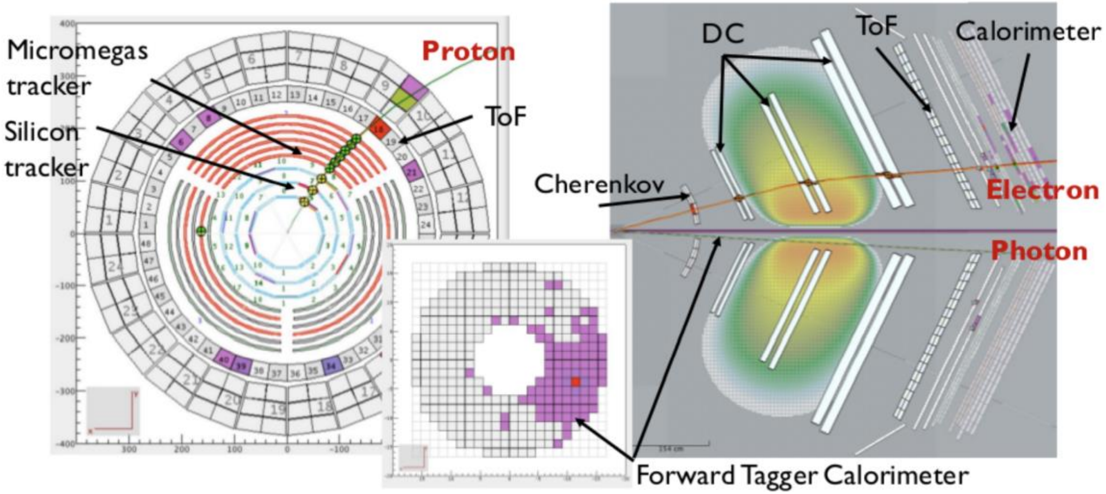

Improving the neutron selection with ML techniques

- The tracking of the CVT is neither 100% efficient nor uniform
- In the dead regions of the CVT protons have no associated track and thus can be misidentified as neutrons
- Protons roughly account for more than >40% contamination in the “nDVCS” signal sample Current approach, based on Machine Learning & Multi-Variate Algorithms:
  - We reconstruct nDVCS from DVCS experiment on proton requiring neutron PID : selected neutron are misidentified protons
  - We use this sample to determine the characteristics of fake neutrons in low- and high-level reconstructed variables
  - Based on those characteristics we subtract the fake neutrons contamination from nDVCS
  - As a « signal » sample in the training of the ML we use $ep \rightarrow en\pi^+$ events from DVCS experiment on proton

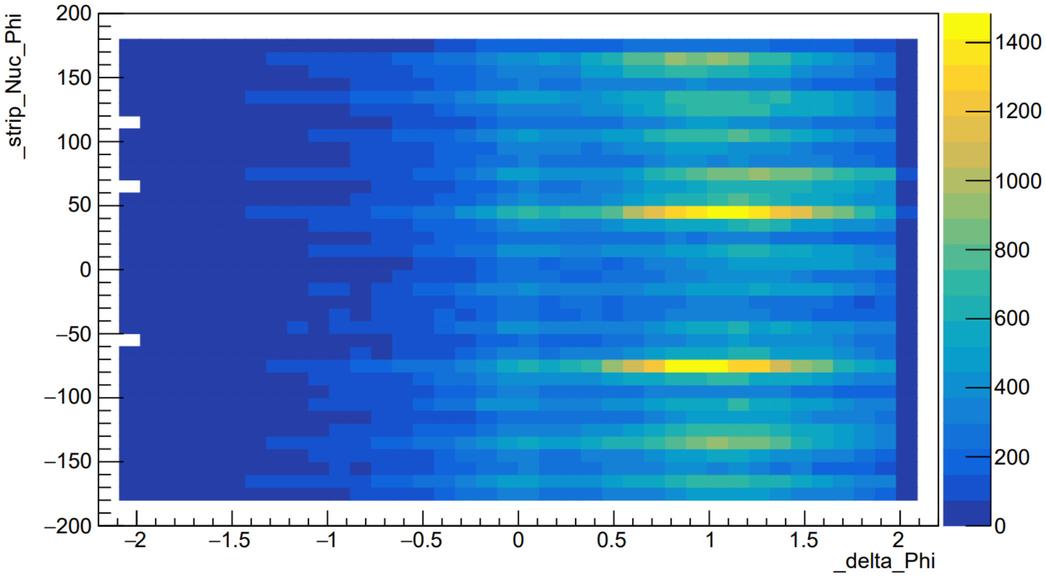

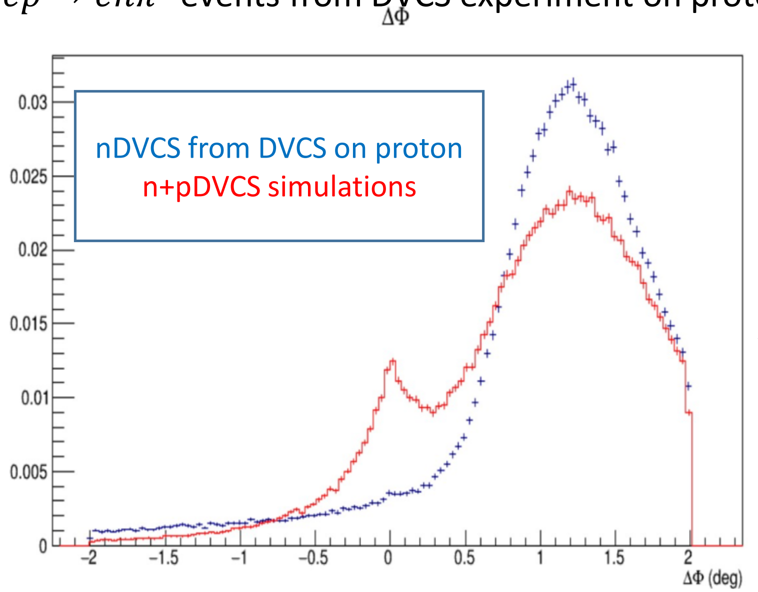

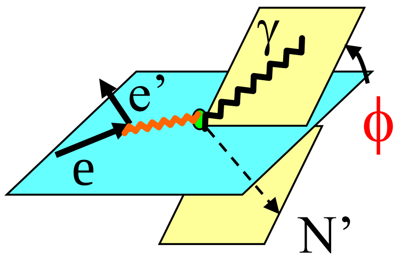

Improving the neutron selection with ML techniques

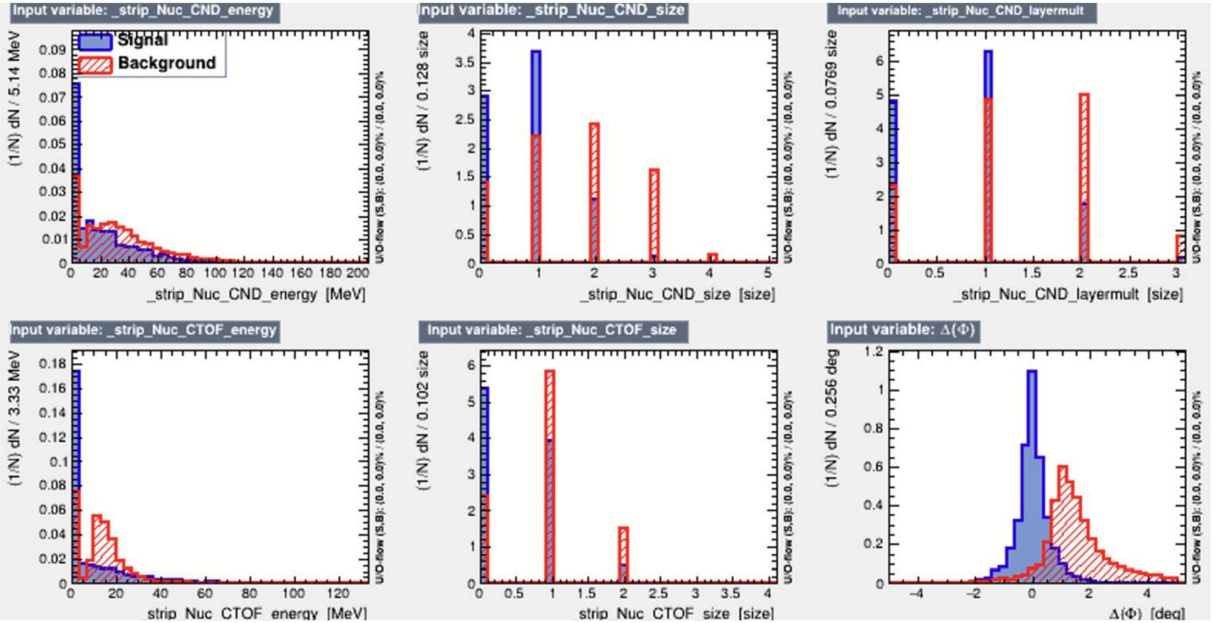

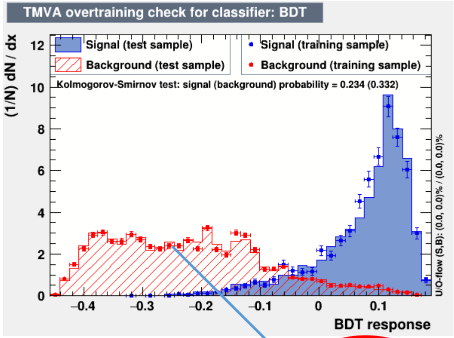

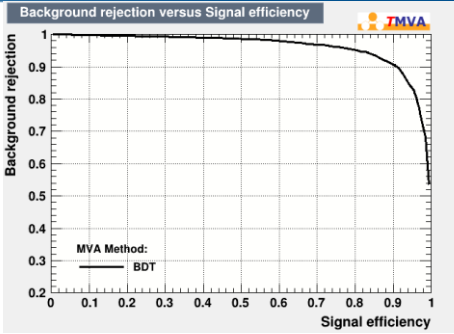

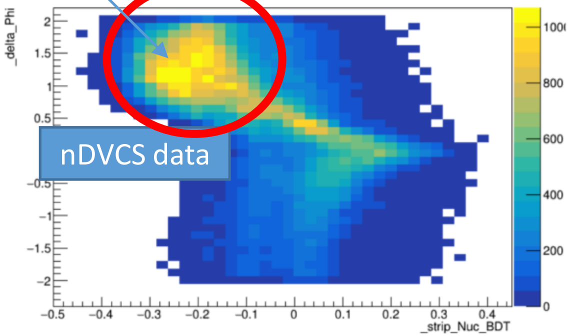

- Using detector variables (CTOF and CND) and one exclusivity variable ($\Delta\Phi$)
- Directly trained on data
- Better optimization of signal to background ratio than straight cuts
- Few percent irreducible contamination corrected for in the final BSA

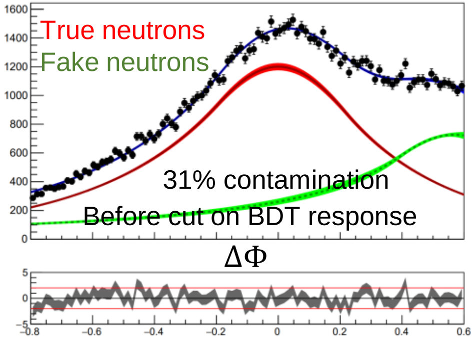

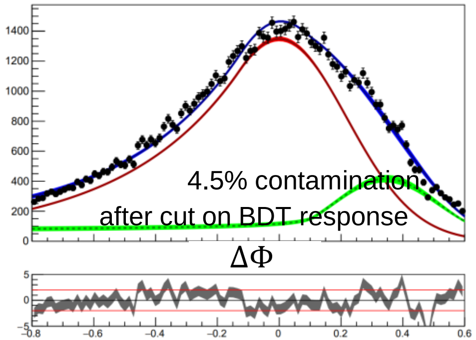

CLAS12: DVCS with an unpolarized deuterium target

- The nDVCS (pDVCS) final state is selected with the following exclusivity criteria: (N:nucleon)
  - Missing mass
    - e d → e N γ X
    - e N → e N γ X
    - e N → e N X
  - Missing momentum
    - e d → e N γ X
  - ΔΦ, Δt, θ(γ,X)
    - Difference between two ways of calculating Φ and t
    - Cone angle between measured and reconstructed photon
- Exclusivity selection is optimized with a 4-D χ^2-like distribution including ΔΦ, Δt, θ(γ,X) and missing mass e N → e N X

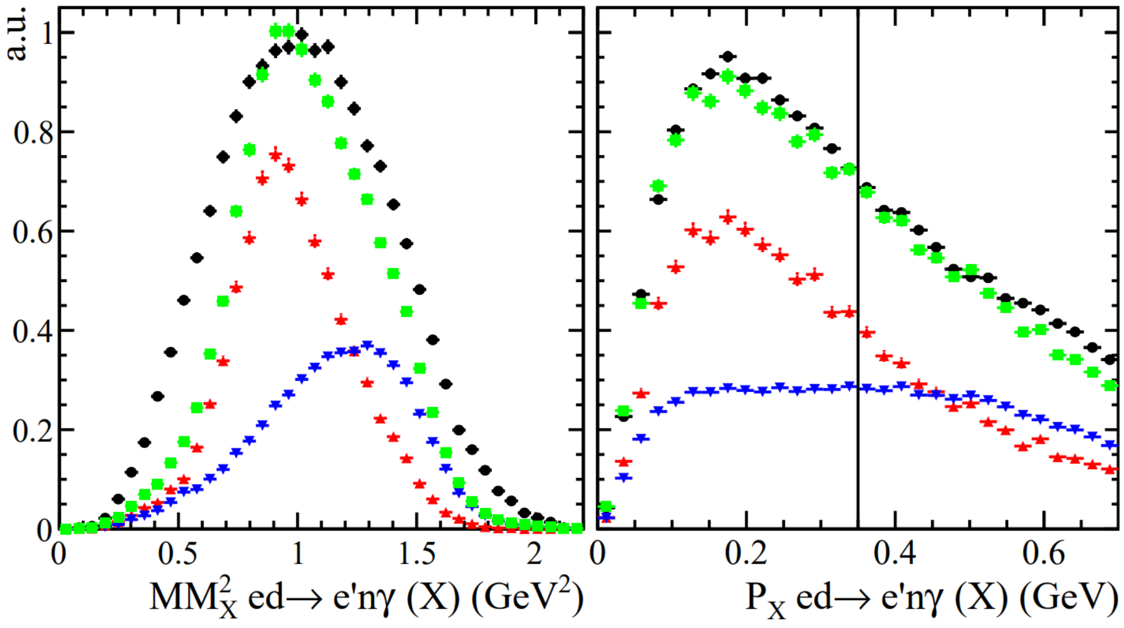

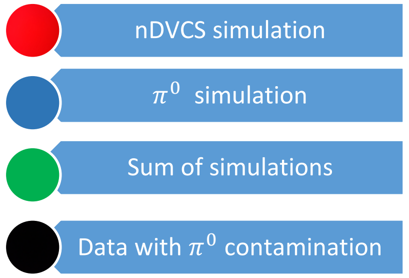

π^0 background contamination is estimated using simulations

π^0 background subtraction

- Subtraction using simulations of the background channel
  - Monte Carlo simulations:
    - GPD-based event generator for DVCS/pi0 on deuterium
    - DVCS amplitude calculated according to the BKM formalism
    - Fermi-motion distribution evaluated according to Paris potential

1. Estimate the ratio of partially reconstructed eN π^0(1 photon) decay to fully reconstructed eN π^0 decays in MC
2. This is done for each kinematic bin to minimize MC model dependence
3. Multiply this ratio by the number of reconstructed eN π^0 in data to get the number of eN π^0(1 photon) in data
4. Subtract this number from DVCS reconstructed decays in data per each kinematical bin

$$\text{Simulations: R} = \frac{\mathrm{N}\left(\mathrm{e}N\pi^0_{1\gamma}\right)}{N(eN\pi^0)}$$

$$\text{Data: } N\left(eN\pi^0_{1\gamma}\right) = R * N(eN\pi^0)$$

$$N(DVCS) = N(DVCS_{recon}) - N(eN\pi^0_{1\gamma})$$

- π^0 background subtraction is also performed by statistical unfolding of contribution to the missing mass spectrum

M. Pivk and F.R. Le Diberder, NIMA 555 1 2005

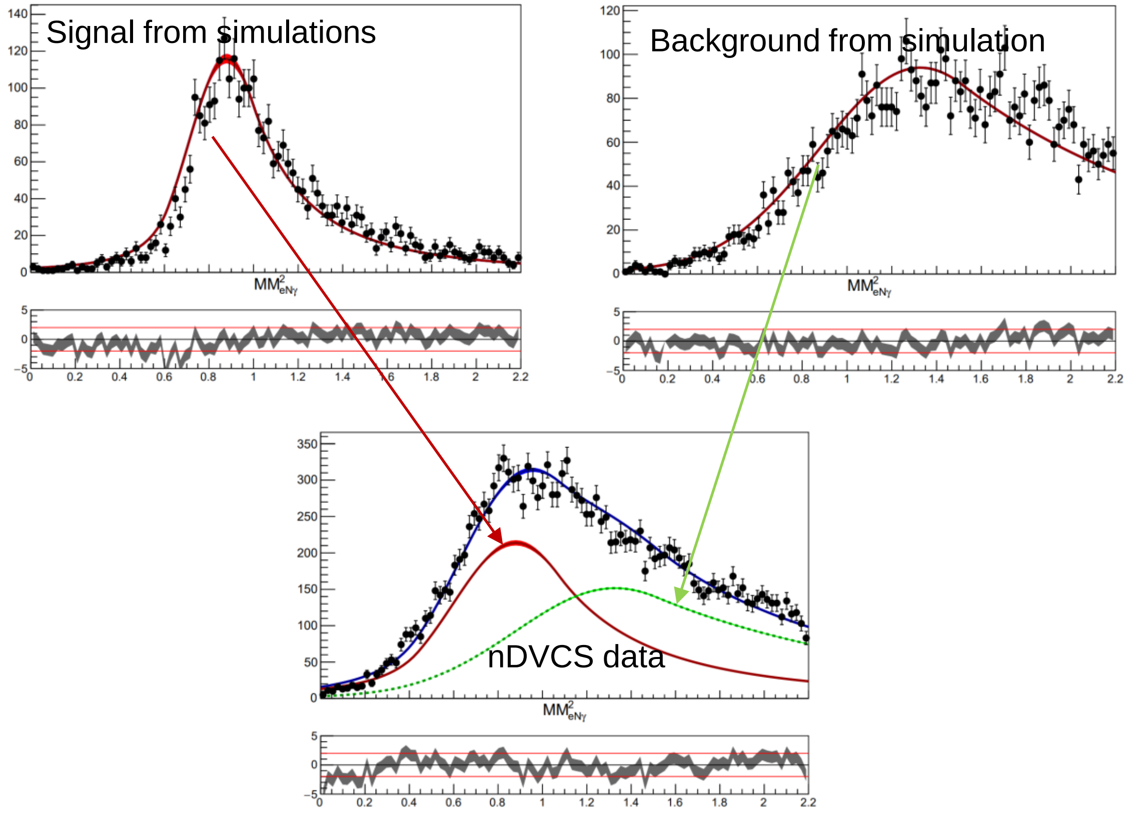

The difference between the estimations of background from both methods is considered as a systematic

First-time measurement of nDVCS with detection of the active neutron

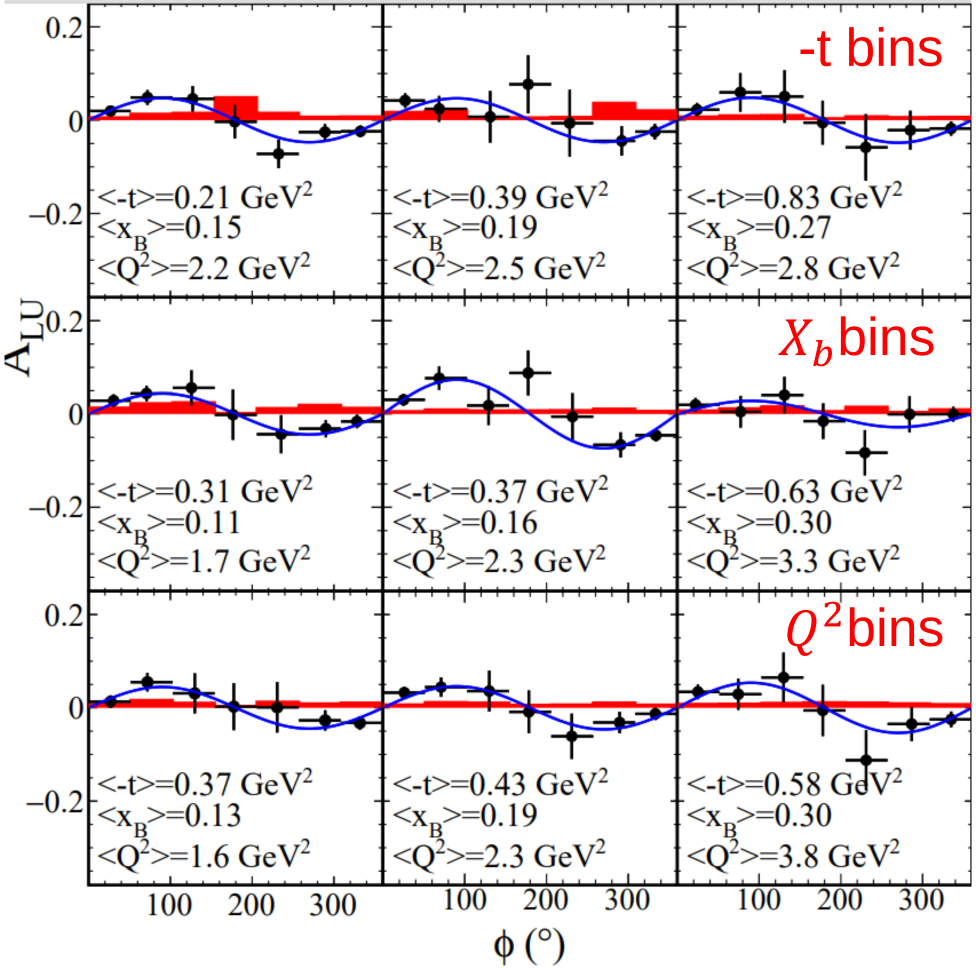

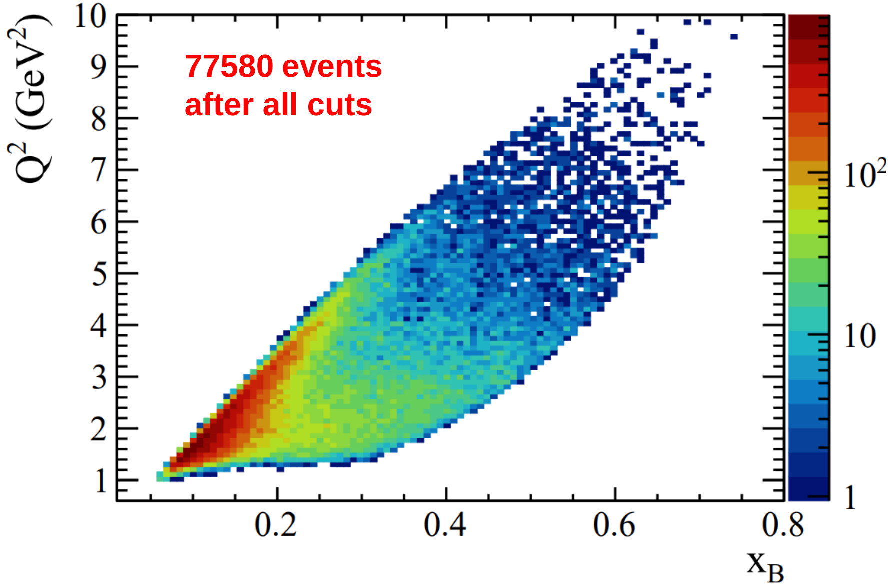

- Compared to the previous experiment, CLAS12 provides :
  - The possibility to scan the BSA of nDVCS on a wide phase space
  - The possibility to reach the high Q^2 high x_b region of the phase space
  - Exclusive measurement with the detection of the active neutron
- Hall A @ JLAB: one measured kinematical point at Q^2=1.9 GeV^2 and x_B=0.36

- Observation of positive BSA for nDVCS
- Systematic errors include:
    - Error due to beam polarization
    - Error due to selection cuts
    - Error due to residual proton contamination
    - Error due to merging of data sets with different energies
- Statistics is expected to double with remaining schedualed beam time and improvements with reconstruction software

$$A_{LU} \approx \Im\{F_1 \boldsymbol{H} + \xi(F_1 + F_2)\widetilde{\boldsymbol{H}} - k\, F_2 \boldsymbol{E} + \ \dots\}$$

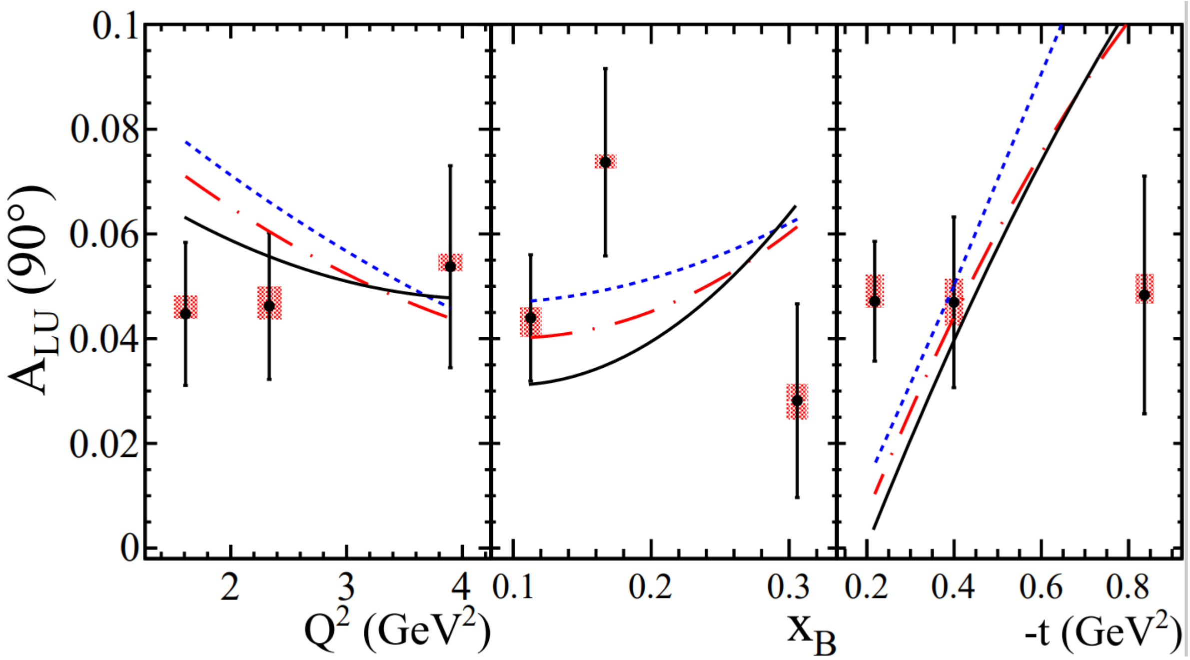

VGG model predictions giving the smallest χ^2

Ju = 0.35 Jd= 0.05
Ju = −0.2 Jd= 0.15
Ju = −0.45 Jd= 0.2

M. Vanderhaeghen, P.A.M. Guichon, and M. Guidal, PRD 60, 094017 (1999)

Deeply Virtual Compton Scattering with an unpolarized deuterium target

- Previous pioneering measurement of nDVCS (Jlab Hall A @ 6 GeV)
  - Beam-energy « Rosenbluth » separation of nDVCS CS using an LD2 target and two different beam energies
  - First observation of non-zero nDVCS CS
- No neutron detection

$$D(e,e'\gamma)X - H(e,e'\gamma)X = n(e,e'\gamma)n + d(e,e'\gamma)d + \ldots$$

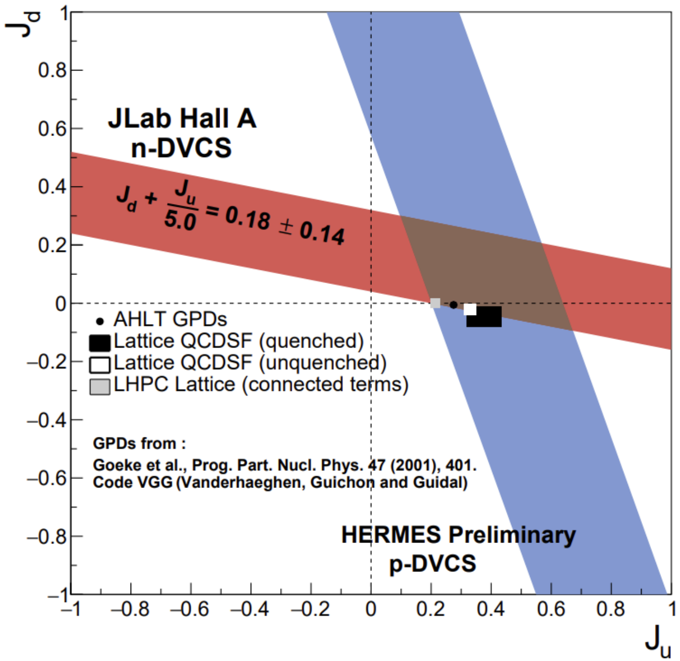

+data from: Mazouz, M. et al. Phys. Rev. Lett. 99, 242501 (2007).

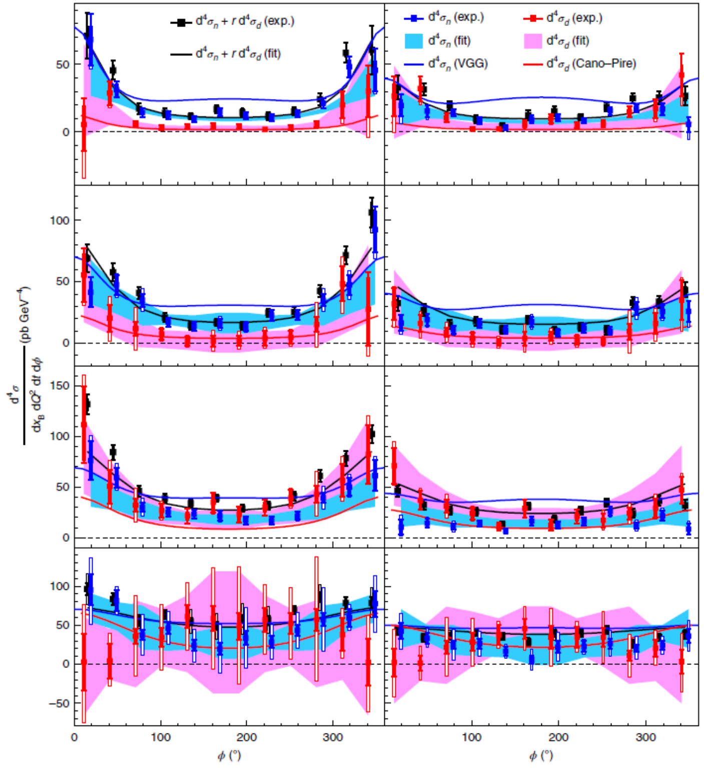

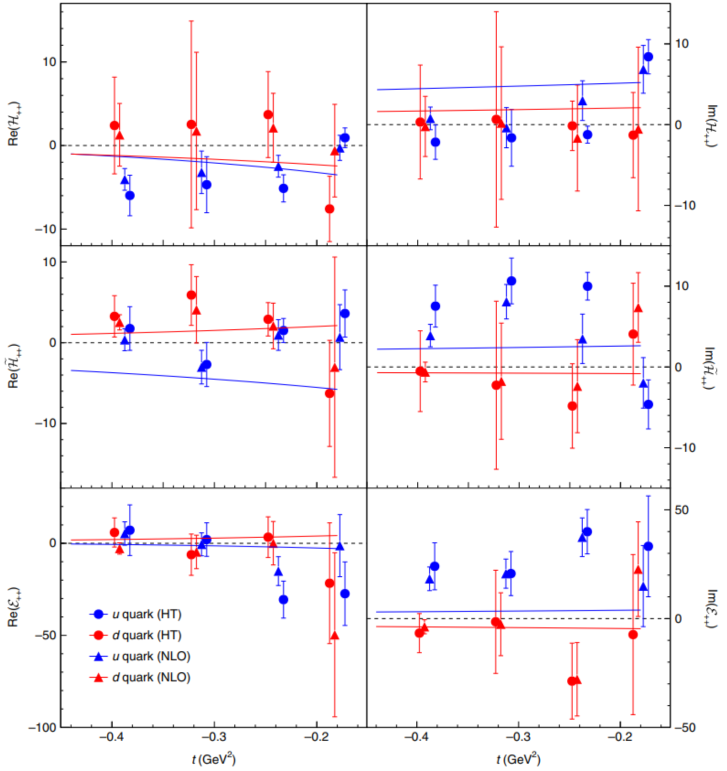

Q^2=1.9 GeV^2 and x_B=0.36

Benali, M., Desnault, C., Mazouz, M. *et al. Nat. Phys.* **16,** 191–198 (2020)

Previously on CFF extraction and flavor separation!

M. Čuić K. Kumericki et al. PhysRevLett.125.232005 and arxiv 2007.00029 (2020)

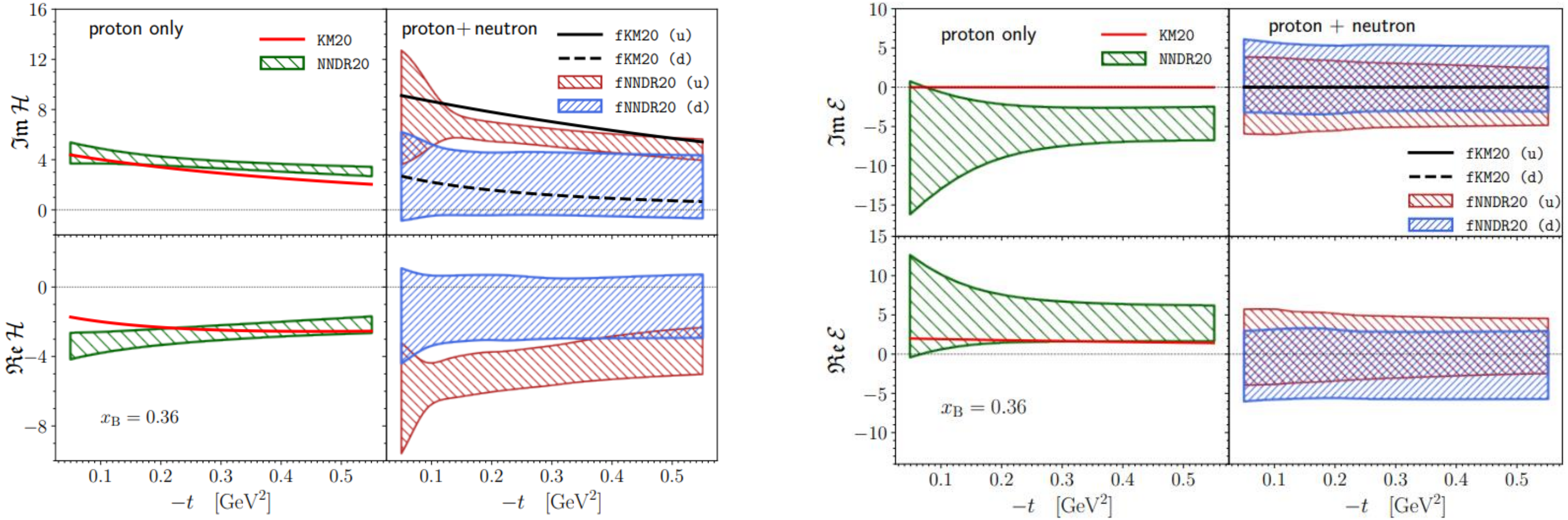

- Proton and neutron data from Jlab (clas6 and Hall A)
  - Up and down contributions to CFF H separated
- CFF E flavors are not separated, a significant sign ambiguity remains

Impact of nDVCS data

- Model-dependant extraction of J_u and J_d
  - Use VGG model (PRD 60, 094017 (1999)) and generate a set of values for J_u and J_d
  - Look for the 1 standard deviation error ellipse: defined as $\chi^2 - \chi^2_{min} = 1$
- Compatible with limits set before by pioneering Hall A measurement
- Compatible with Lattice QCD predictions
- Shortcomings:
  - none of the considered sets of J_u and J_d reproduce correctly the distributions
  - VGG has problems in reproducing proton data
- Closest-to-truth model-dependent representation of data.

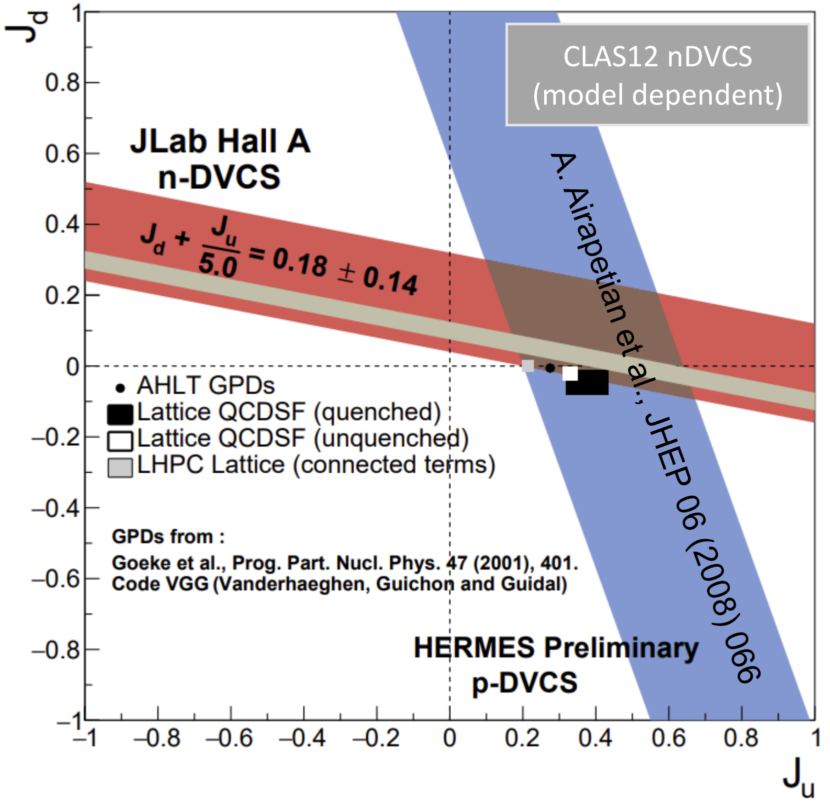

Today on CFF extraction and flavor separation!

- Global fits of CFF using neural networks (model-independent)
  - K. Kumericki et al., JHEP 07, 073531 (2011); M. Cuic, K. Kumericki, et al., Phys. Rev. Lett. 533 125, 232005 (2020)).
- Data used:
  - CLAS6 and HERMES pDVCS observables
  - CLAS12 pDVCS BSA and nDVCS BSA
- Same extraction method applied to nDVCS Hall-A data, only separation for ImH

Clear quark-flavor separation of both ImH and ImE thanks to CLAS12 nDVCS data allow the

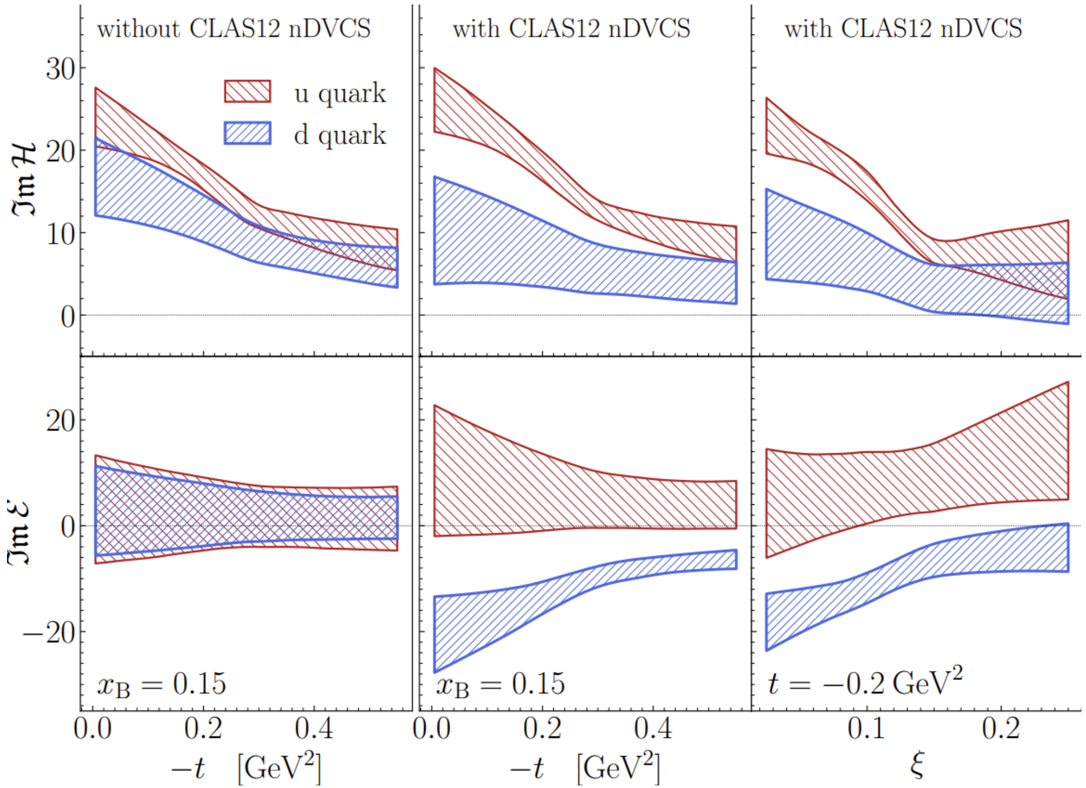

Today on CFF extraction and flavor separation!

- Global fits of CFF using neural networks (model-independent)
  - K. Kumericki et al., JHEP 07, 073531 (2011); M. Cuic, K. Kumericki, et al., Phys. Rev. Lett. 533 125, 232005 (2020)).
- Data used:
  - CLAS6 and HERMES pDVCS observables
  - CLAS12 pDVCS BSA and nDVCS BSA
- Same extraction method applied to nDVCS Hall-A data, only separation for ImH

Clear quark-flavor separation of both ImH and ImE thanks to CLAS12 nDVCS data allow the

Results extrapolated to t=0 GeV^2

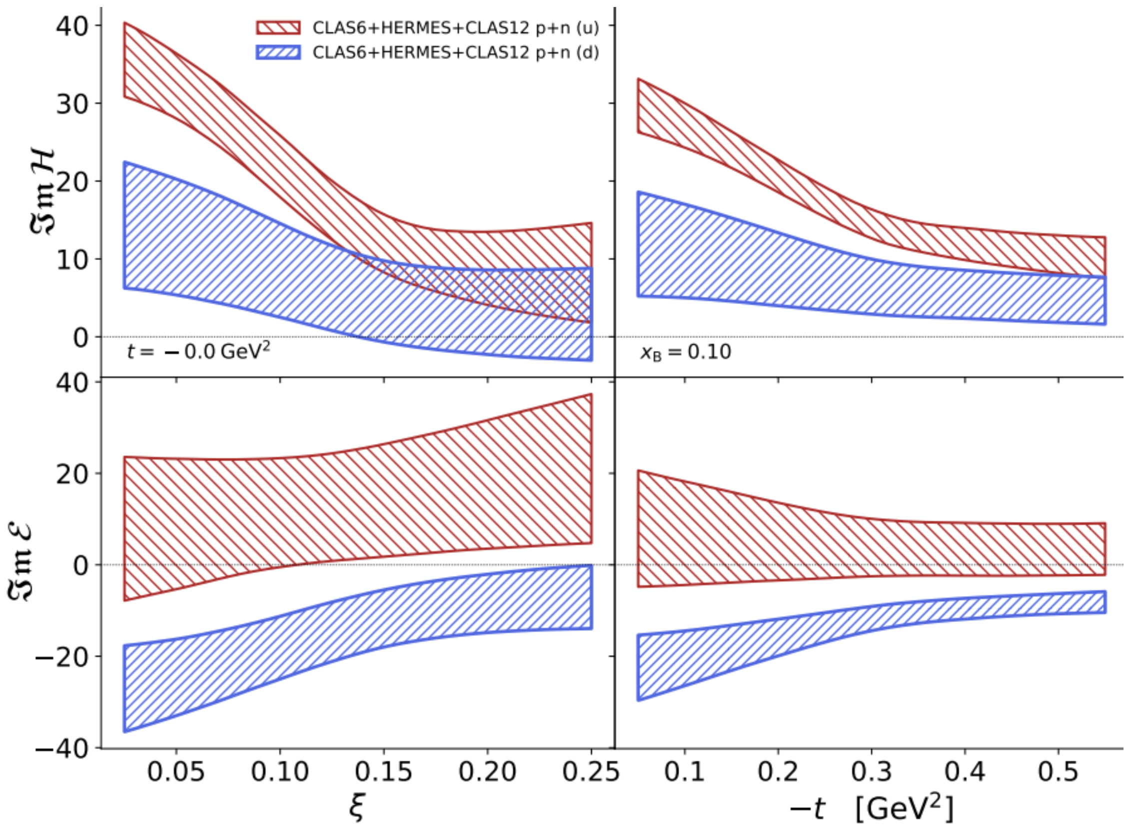

CLAS12: pDVCS with an unpolarized deuterium target

First-time measurement of incoherent pDVCS on deuteron

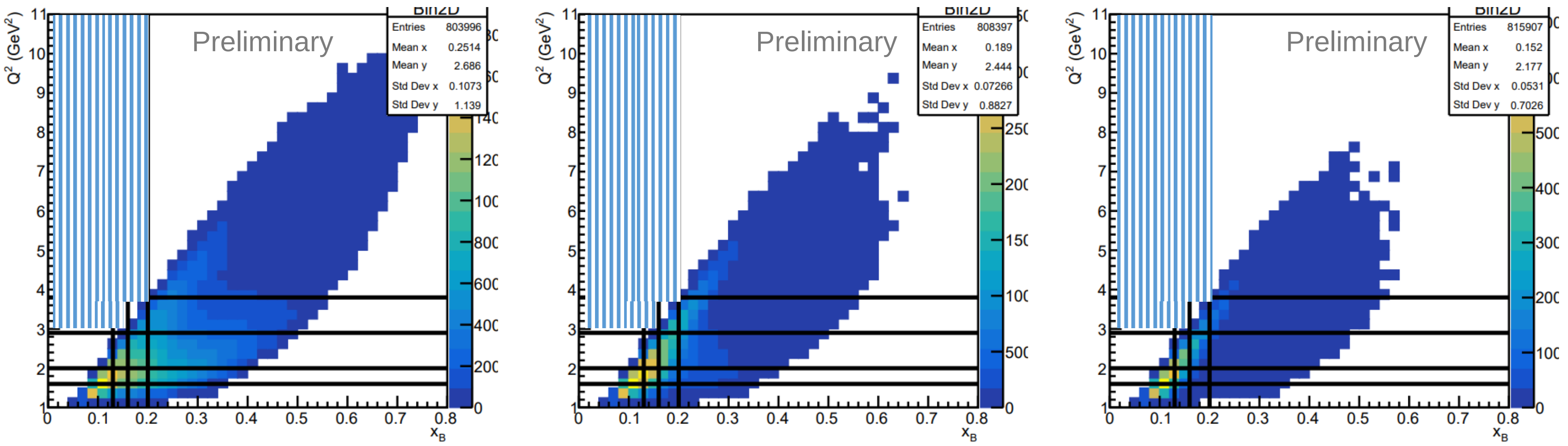

Bin numbering starts from left to right and from bottom up

bin number	$< Q^2 >$ GeV^2	$< x_b >$	$< -t >$ GeV^2
1	1.43794	0.10069	0.767361
2	1.48186	0.144366	0.844629
3	1.4914	0.178824	0.87073
4	1.50756	0.2373	0.851789
5	1.76792	0.114657	0.777427
6	1.8051	0.144373	0.825599
7	1.80447	0.179402	0.863781
8	1.81536	0.258406	0.923301
9	2.0849	0.124705	0.764681
10	2.26532	0.146577	0.793068
11	2.4122	0.179697	0.827414
12	2.43479	0.287563	1.00085
13	3.0799	0.188297	0.790217
14	3.31486	0.30929	1.04349
15	4.83889	0.380624	1.228
16	1.43915	0.100179	0.356721
17	1.49262	0.142616	0.362959
18	1.4954	0.176071	0.350067
19	1.50509	0.249393	0.309281
20	1.77057	0.114679	0.34701
21	1.81394	0.143668	0.348841
22	1.82669	0.175209	0.355866
23	1.81383	0.263491	0.318227
24	2.08646	0.124711	0.342502
25	2.26728	0.146758	0.340636
26	2.46209	0.17752	0.348786
27	2.45997	0.26518	0.340427
28	3.08043	0.188274	0.334151
29	3.34394	0.248423	0.35341
30	4.46623	0.295696	0.370628
31	1.43626	0.0986234	0.200339
32	1.50515	0.13983	0.218898
33	1.49559	0.17749	0.195675
34	1.50618	0.241843	0.211988
35	1.77032	0.114665	0.198266
36	1.83854	0.140417	0.212787
37	1.82375	0.176723	0.20719
38	1.81611	0.248591	0.216637
39	2.08516	0.124803	0.198108
40	2.27128	0.145977	0.203877
41	2.55103	0.174046	0.21458
42	2.44112	0.256179	0.228055
43	3.07532	0.187944	0.210093
44	3.37468	0.230834	0.230575
45	4.30035	0.274016	0.247191

- Complementary to previous experiment on proton target:
  - Quantify medium effects on GPDs

CLAS12: pDVCS with an unpolarized deuterium target

- Systematic errors include:
  - Error due to beam polarization
  - Error due to selection cuts
  - Error due to merging of data sets with different energies
- Statistics is expected to triple with remaining schedualed beam time and improvements with reconstruction software

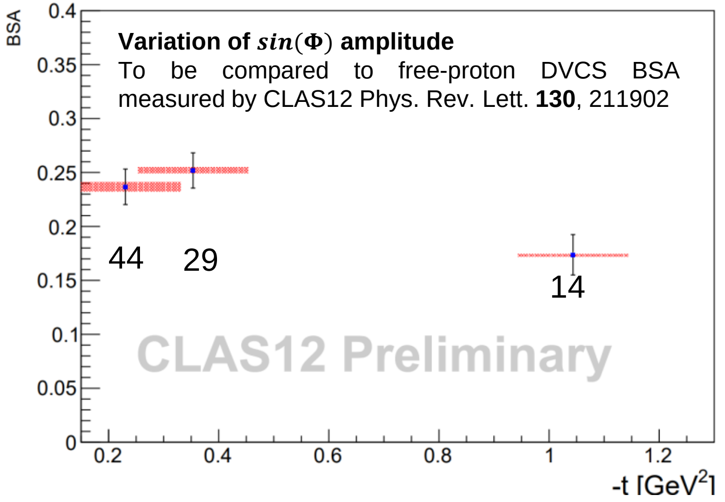

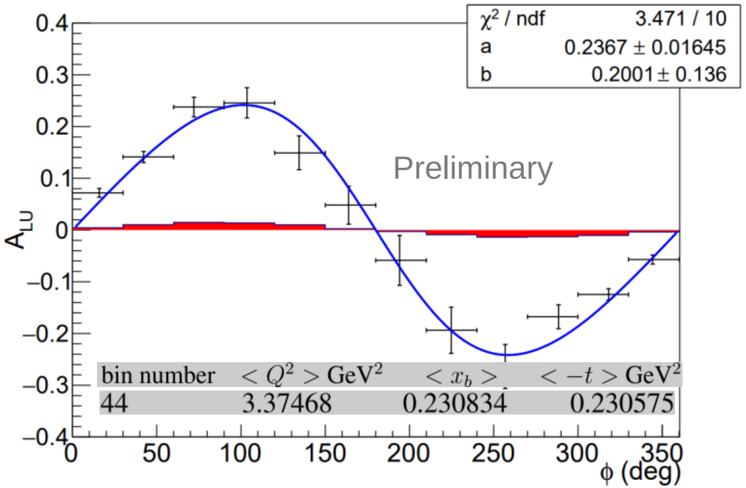

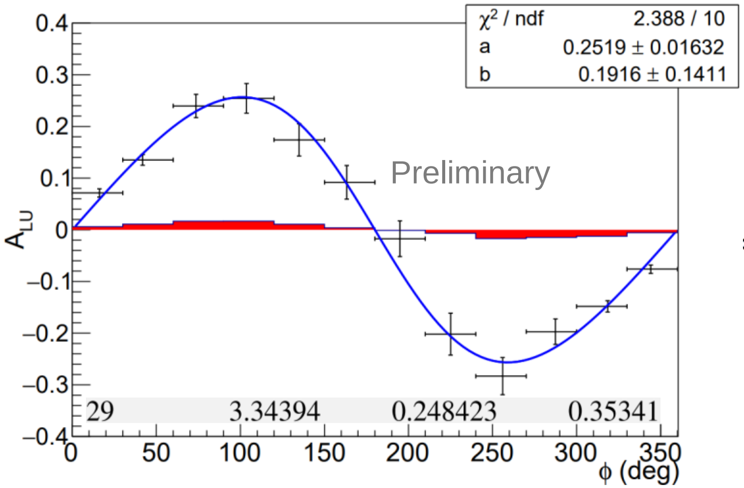

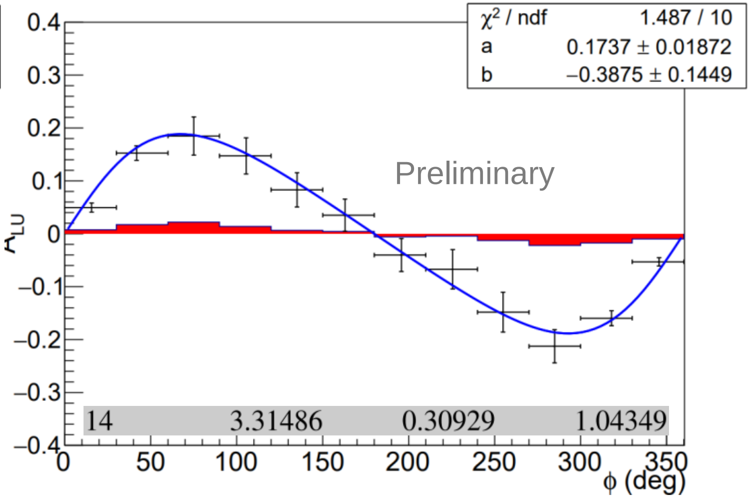

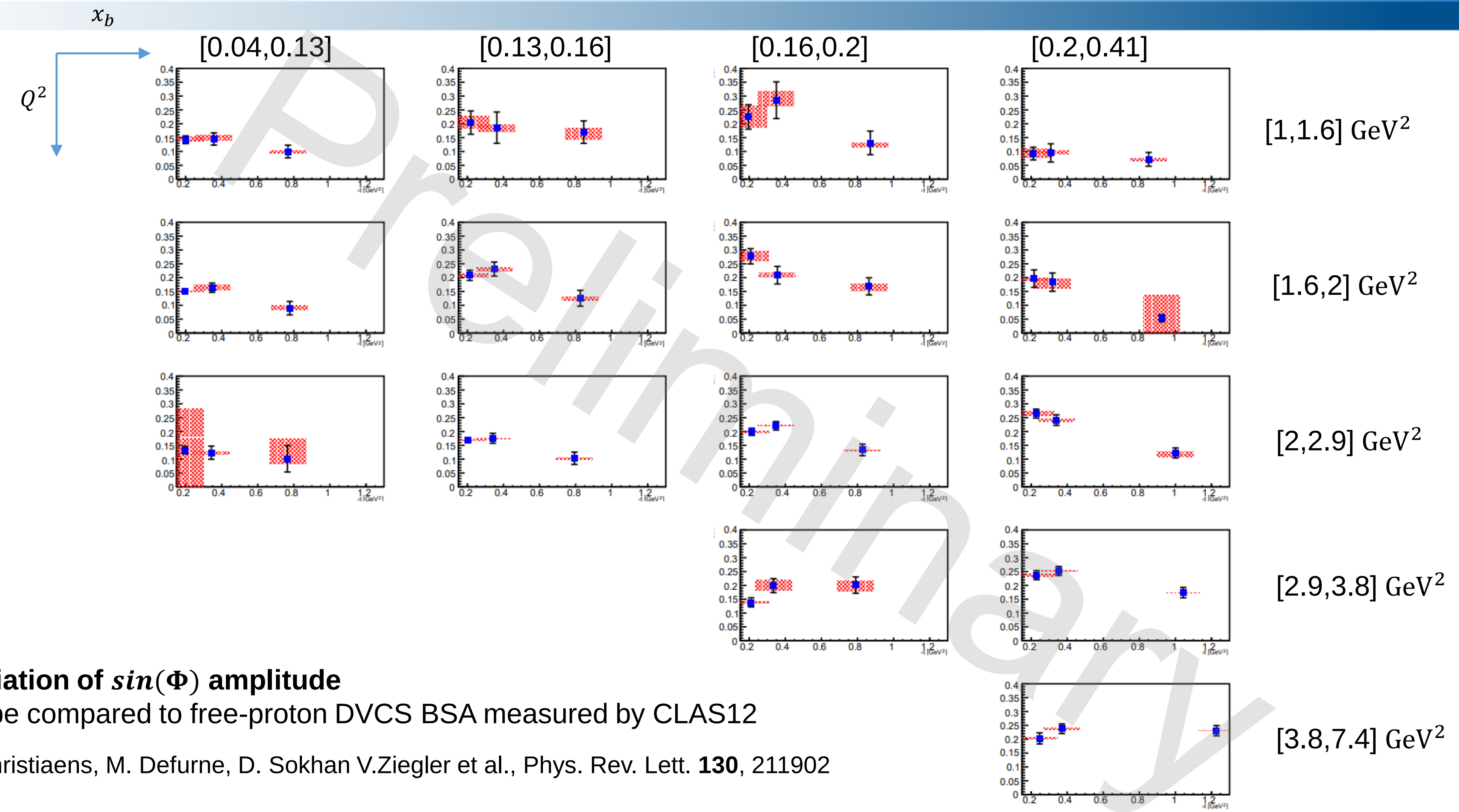

Variation of $sin(\Phi)$ amplitude

To be compared to free-proton DVCS BSA measured by CLAS12

G. Christiaens, M. Defurne, D. Sokhan V.Ziegler et al., Phys. Rev. Lett. **130**, 211902

- Reanalysis of proton DVCS data (on hydrogen) is under review by the collaboration
  - Use of Machine Learning to optimize process selection

$ep \rightarrow e\gamma p$: **BDT**

To optimize the DVCS event selection, a Boosted Decision Tree (BDT) is trained to classify the events.

- Discriminating variables: $\{M^2_{ep\gamma}, M^2_{e\gamma}, \Delta\phi, \Delta t, \theta_{\gamma X}\}$.
- Simulated DVCS as signal.
- Simulated π^0 events, reconstructed as DVCS, as background.

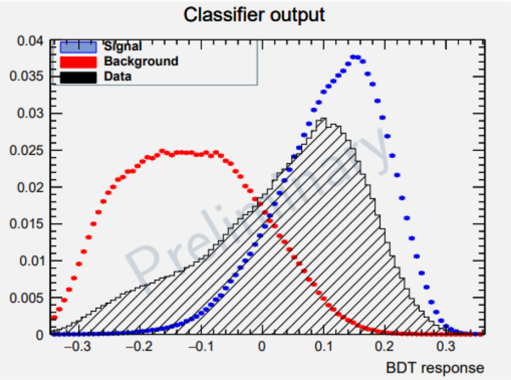

(a) BDT output distributions for different datasets.

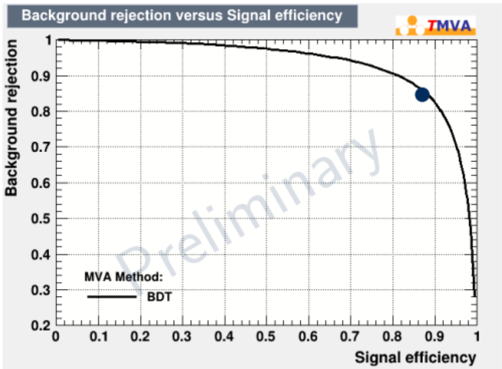

(b) ROC curve of the model and applied cut.

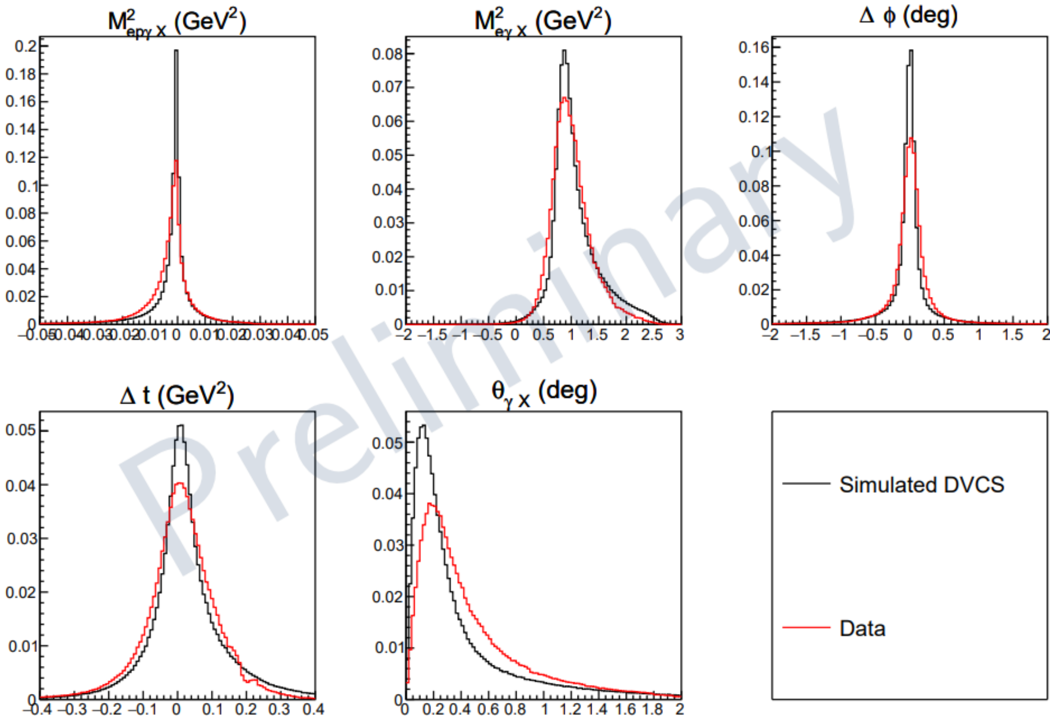

pDVCS on Hydrogen revisited analysis done by J.S. Alvarado

- Reanalysis of proton DVCS data (on hydrogen) is under review by the collaboration
  - Use of Machine Learning to optimize process selection
  - Ignore proton information to increase phase-space

There is an important increase on statistics

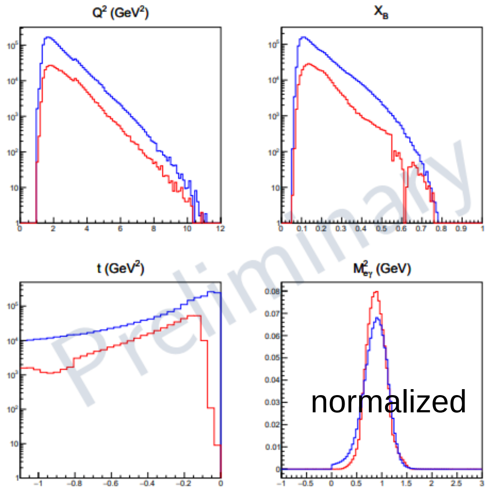

Figure: Kinematic variables for the analysis with proton (red) and without proton (blue) information.

We access a wider region in t**.**

Chosen bin*: $1.8 < Q^2(\text{GeV}^2) < 2.4,\ 0.16 < x_B < 0.26,\ -t(\text{GeV}^2) < 0.2$

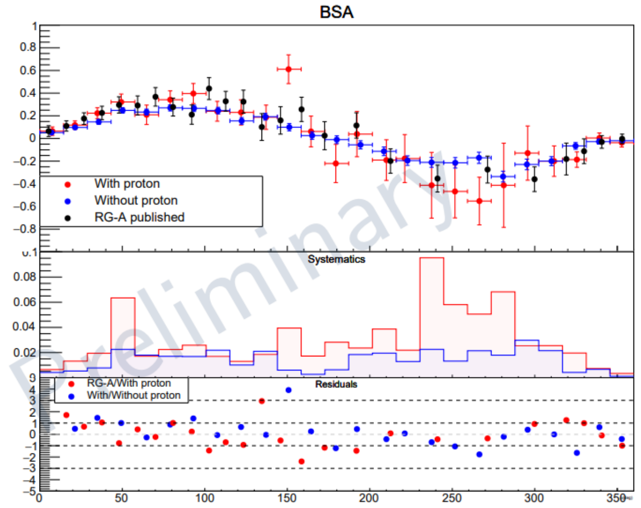

- The analysis of absolute DVCS cross section on proton is advanced (Sangbaek Lee)
  - No release plots but analysis in advanced stage
- A parallel analysis of DVCS absolute cross section (ignoring proton detection) is just starting (J.S. Alvarado)
- Another nDVCS experiment on longitudinally polarized deuterium target was carried out in 2022 -2023 with CLAS12 (analysis by N. Pilleux)
- The second half of Run Group B will run with double luminosity following the CLAS12 high-lumi upgrade
- A transversely polarized target pDVCS experiment is foreseen for ~2028 with CLAS12
- The combination of all neutron and proton DVCS data will allow quark-flavor separation of all CFFs in the valence region
- The Ji's sum rule is the ultimate, ambitious goal of this program

Observable (target)	CFF sensitivity	Status
lTSA(p), lDSA(p)	$\Im\{\boldsymbol{H_p}, \boldsymbol{\tilde{H}_p}\}, \Re\{\boldsymbol{H_p}, \boldsymbol{\tilde{H}_p}$	Data taken
lTSA(n), lDSA(n)	$\Im\{\boldsymbol{H_n}\}, \Re\{\boldsymbol{H_n}\}$	Data taken
tTSA(p)	$\Im\{\boldsymbol{H_p}\}, \Im\{\boldsymbol{E_p}\},$	~2028

- Analysis ongoing: Deuteron DVCS
  - Phyisics observable to extract is Beam Spin Asymmetry (BSA)

$$\Delta\sigma_{LU} \sim \sin(\phi)\,\Im\left\{\frac{2G_1\boldsymbol{H_1} + (G_1 - \tau G_3)(\boldsymbol{H_1} - 2\tau\boldsymbol{H_3}) + \frac{2}{3}\tau G_3\boldsymbol{H_5}}{2G_1^2 + (G_1 - 2\tau G_3)^2}\right\}$$

  - Spin 1: 9 GPDs for each quark flavor
    - BSA of DVCS off deuterium is sensitive to 3 of them

Summary

- GPDs are powerful tool to explore the structure of the nucleons and nuclei
  - Nucleon tomography, quark angular momentum, distribution of forces in the nucleon
- Exclusive reactions can provide important information on nucleon structure
  - DVCS via the extraction of GPDs
- CLAS12 offers a wide kinematical reach over which the GPDs dependence on different kinematical variables can be scanned
  - Data to add constraints on GPDs in unexplored regions of the phase space
  - Possibilities to measure new observables using different experimental configurations
    - Flavor separation of GPDs
- Promising results from incoherent DVCS on deuteron (n and p channels) from CLAS12 data
  - First BSA measurement from neutron-DVCS with tagged neutron
  - First measurement of BSA for proton-DVCS with deuterium target
    - To be compared to free-proton DVCS BSA measured by CLAS12

G. Christiaens, M. Defurne, D. Sokhan V.Ziegler et al., Phys. Rev. Lett. 130 (21) 211902 (2023)

Conclusions and outlook

- The beam -spin asymmetry for nDVCS is a precious tool to constrain the GPD E and for quark -flavor separation of GPDs
- CLAS12 measured the BSA for nDVCS with detected neutron for the first time
- The first ~43% of the experiment ran in 2019 -2020 at Jlab
- A small but clear BSA was extracted
- Comparison with a model allows to put model-dependent constraints on J_d
- The data, together with the proton DVCS data, allow the quark -flavor separation of ImH and ImE
- An article is ready for submission to PRL

arXiv:2406.15539

First Measurement of Deeply Virtual Compton Scattering on the Neutron with Detection of the Active Neutron

A. Hobart,[1] S. Niccolai,[1] M. Čuić,[2] K. Kumerički,[2] P. Achenbach,[3] J.S. Alvarado,[1] W.R. Armstrong,[4] H. Atac,[5] H. Avakian,[3] L. Baashen,[6,*] N.A. Baltzell,[3] L. Barion,[7] M. Bashkanov,[8] M. Battaglieri,[3,9,†] B. Benkel,[10] F. Benmokhtar,[11] A. Bianconi,[12,13] A.S. Biselli,[14] S. Boiarinov,[3] M. Bondi,[15] W.A. Booth,[8] F. Bossù,[16] K.-Th. Brinkmann,[17] W.J. Briscoe,[18] W.K. Brooks,[19] S. Bueltmann,[20] V.D. Burkert,[3] T. Cao,[3] R. Capobianco,[21] D.S. Carman,[3] P. Chatagnon,[3,1] G. Ciullo,[7,22] P.L. Cole,[23] M. Contalbrigo,[7] A. D'Angelo,[10,24] N. Dashyan,[25] R. De Vita,[9,‡] M. Defurne,[16] A. Deur,[3] S. Diehl,[17,21] C. Dilks,[3,26] C. Djalali,[27] R. Dupre,[1] H. Egiyan,[3] A. El Alaoui,[19] L. El Fassi,[28] L. Elouadrhiri,[29] S. Fegan,[8] A. Filippi,[30] C. Fogler,[20] K. Gates,[31] G. Gavalian,[3,32] G.P. Gilfoyle,[33] D. Glazier,[31] R.W. Gothe,[34] Y. Gotra,[3] M. Guidal,[1] K. Hafidi,[4] H. Hakobyan,[19] M. Hattawy,[20] F. Hauenstein,[3,20] D. Heddle,[29,3] M. Holtrop,[32] Y. Ilieva,[34,18] D.G. Ireland,[31] E.L. Isupov,[35] H. Jiang,[31] H.S. Jo,[36] K. Joo,[21] T. Kageya,[3] A. Kim,[21] W. Kim,[36] V. Klimenko,[21] A. Kripko,[17] V. Kubarovsky,[3,37] S.E. Kuhn,[20] L. Lanza,[10,24] M. Leali,[12,13] S. Lee,[4,38] P. Lenisa,[7,22] X. Li,[38] I.J.D. MacGregor,[31] D. Marchand,[1] V. Mascagna,[12,39,13] B. McKinnon,[31] Z.E. Meziani,[4] S. Migliorati,[12,13] R.G. Milner,[38] T. Mineeva,[19] M. Mirazita,[40] V. Mokeev,[3,35] C. Muñoz Camacho,[1] P. Nadel-Turonski,[3] P. Naidoo,[31] K. Neupane,[34] G. Niculescu,[41] M. Osipenko,[9] P. Pandey,[38] M. Paolone,[42,5] L.L. Pappalardo,[7,22] R. Paremuzyan,[3,32] E. Pasyuk,[3] S.J. Paul,[43] W. Phelps,[29] N. Pilleux,[1] M. Pokhrel,[20] S. Polcher Rafael,[16] J. Poudel,[3] J.W. Price,[44] Y. Prok,[20] T. Reed,[6] J. Richards,[21] M. Ripani,[9] J. Ritman,[45,46] P. Rossi,[3,40] A.A. Golubenko,[35] C. Salgado,[47] S. Schadmand,[45,46] A. Schmidt,[18] Marshall B.C. Scott,[18] E.M. Seroka,[18] Y.G. Sharabian,[3] E.V. Shirokov,[35] U. Shrestha,[21,27] N. Sparveris,[5] M. Spreafico,[9] S. Stepanyan,[3] I.I. Strakovsky,[18] S. Strauch,[34,18] J.A. Tan,[36] N. Trotta,[21] R. Tyson,[3] M. Ungaro,[3] S. Vallarino,[9] L. Venturelli,[12,13] V. Tommaso,[9] H. Voskanyan,[25] E. Voutier,[1] D.P Watts,[8] X. Wei,[3] R. Williams,[8] M.H. Wood,[48,34] L. Xu,[1] N. Zachariou,[8] J. Zhang,[49] Z.W. Zhao,[26] and M. Zurek[4]
(The CLAS Collaboration)